Review on tube model based constitutive equations for polydisperse linear and long-chain branched polymer melts

Esmaeil Narimissa[1,2,a)] and Manfred H. Wagner[3]

[1]*Department of Chemical Engineering, Technion–Israel Institute of Technology (IIT), Technion City, Haifa 32 000, Israel*
[2]*Department of Chemical Engineering, Guangdong Technion–Israel Institute of Technology (GTIIT), Shantou 515063, China*
[3]*Polymer Engineering / Polymer Physics, Berlin Institute of Technology (TU Berlin), Ernst-Reuter-Platz 1, 10587 Berlin, Germany*

(Received 6 October 2018; final revision received 9 January 2019; published 4 March 2019)

Abstract

Rheological equations of state are of great importance for characterization of polymer melts and for simulation of polymer processing. This concise review considers tube model based constitutive equations developed in the last 40 years since the original publication of Doi and Edwards in 1978. The emphasis is on the concepts, assumptions, and material parameters introduced to model nonlinear viscoelasticity of polydisperse linear and long-chain branched polymer melts. Linear viscoelasticity is assumed to be known, either from linear-viscoelastic modeling or by experimental characterization. The scope is limited to constitutive equations which are based on the linear-viscoelastic relaxation modulus and can be expressed in terms of integral, differential, or integro-differential equations.

Multimode models based on the concept of preaveraged stretch require a large number of nonlinear model parameters. Relaxing the assumption of a constant tube diameter, the number of nonlinear model parameters can be drastically reduced to 2 or 3, independent of the number of Maxwell modes needed to represent the linear viscoelasticity. https://doi.org/10.1122/1.5064642

I. INTRODUCTION

The nonlinear rheological behavior of polymers occurs in response to large and/or fast deformations when the Boltzmann superposition principle becomes unable to predict the rheological behaviors in terms of linear viscoelasticity. There is no single universal constitutive equation nor rheological equation of state capable of modeling all nonlinear behaviors, and proposed constitutive equations are either based on continuum mechanics considerations or are mesoscopic molecular models taking into account fundamental aspects of macromolecular systems such as uncrossability and architecture of polymer chains [1]. Rheological equations of state are of great importance in the characterization of polymer systems as they allow reducing the complex rheological behavior to a unique set of rheological parameters. They are equally important in the simulation of polymer processes and in understanding the effects of processing on the properties of polymeric materials. Microscopic molecular or atomistic models are not in the scope of this review, as their predictions are accessible only by numerical simulations and can usually not be presented in terms of closed form constitutive equations. On the other hand, models derived solely from continuum mechanics principles are empirical in the sense that they do not take into account the specific nature of the material considered. However, as the molecular structure of polymer melts (e.g., molar mass, polydispersity, and chain architecture) plays the primary role in determining their rheological properties, constitutive equations based on mesoscopic molecular modeling are of significant importance in rheology. In particular, the tube-based models have been able to reflect fundamental molecular aspects of polymers through averaging the effect of neighboring chains on the test chain via a mean-field approach.

This review considers tube model based constitutive equations developed for the prediction of the nonlinear rheology of polydisperse linear and long-chain branched (LCB) polymer melts. The rheology of polydisperse polymers is of great interest to the polymer processing industry, as most commercial polymers are polydisperse. The emphasis is thus on the concepts, assumptions, and material parameters introduced to model nonlinear viscoelasticity as well as on the application of these models in the simulation of polymer processes. The linear-viscoelastic behavior, which can be expressed fully and uniquely by, e.g., the linear-viscoelastic relaxation modulus, is assumed to be known, either from linear-viscoelastic modeling or by experimental characterization. The scope is limited to the nonlinear constitutive equations, which are based on the relaxation modulus, and can be expressed in terms of integral, differential, or integro-differential equations.

II. THE TUBE MODEL OF DOI AND EDWARDS

The tube model of Doi–Edwards (DE) [2–5] was originally developed for monodisperse linear polymers based on

a)Author to whom correspondence should be addressed; electronic mail: esmaeiln@technion.ac.il

the idea of the reptating motion of a linear entangled chain with molar mass M in a tube with equilibrium contour length of $L_0 = Na_0$, where N is the number of primitive path steps connecting two consecutive entanglements and a_0 is the tube diameter. The tube concept is based on the hypothetical view of a test chain laterally confined in a mesh of constraints created by the surrounding chains having the same molar mass as the test chain. Upon deformation, the recovery of the contour length of the primitive chain (i.e., relaxation) occurs due to the reptation (chain diffusion) and retraction mechanisms. As originally described by de Gennes [6], during reptation, the test chain escapes from the tube by sliding back and forth within the tube until completely moves its mass out of the tube. The relaxation time associated with the reptation mechanism is the disengagement (or reptation) time $\tau_d \propto M^3$. During the fast retraction mechanism, the contour length is recovered after a Rouse relaxation process governed by the Rouse time $\tau_R \propto M^2$. According to one of the basic hypotheses of the tube theory, the tension in the deformed chain equates with its equilibrium value even in the nonlinear viscoelastic regime, which is commensurate with the assumption that the tube diameter a_0 does not change with deformation and remains constant. The segmental tube orientation is the main contributor to the extra-stress tensor $\boldsymbol{\sigma}$, and if expressed as a single integral constitutive equation, is given by

$$\boldsymbol{\sigma}(t) = \int_{-\infty}^{t} \frac{\partial G(t-t')}{\partial t'} \mathbf{S}_{\mathrm{DE}}^{\mathrm{IA}}(t,t')dt'. \tag{1}$$

It should be noted that strictly speaking Eq. (1) is an approximation, as the "full" DE model cannot be expressed by integral equation. The strain tensor $\mathbf{S}_{\mathbf{DE}}$ is given by

$$\mathbf{S}_{\mathrm{DE}}^{\mathrm{IA}}(t,t') = \frac{15}{4}\frac{1}{\langle u' \rangle}\left\langle \frac{\mathbf{u}'\mathbf{u}'}{u'} \right\rangle. \tag{2}$$

Here, $\langle\rangle$ is the average over an isotropic distribution function of unit vector $\mathbf{u}$ described as a surface integral over unit sphere [4],

$$\langle\rangle \equiv \frac{1}{4\pi}\oiint [\,] \sin\theta_0 d\theta_0 d\varphi_0. \tag{3}$$

$\mathbf{u}'$ is the deformed unit vector $\mathbf{u}$ with the length u' defined from the affine deformation hypothesis,

$$\mathbf{u}'(t,t') = \mathbf{F}_t^{-1}(t,t').\mathbf{u}(t'), \tag{4}$$

where $\mathbf{F}_t^{-1}$ denotes the deformation gradient tensor.

Based on the independent alignment (IA) approximation of DE theory, the tube segments are assumed to be aligned independently in the field of flow, and the strain tensor in Eq. (1) is replaced by

$$\mathbf{S}_{\mathrm{DE}}^{\mathrm{IA}}(t,t') \equiv 5\left\langle \frac{\mathbf{u}'\mathbf{u}'}{u'^2} \right\rangle = 5\mathbf{S}(t,t'), \tag{5}$$

where $\mathbf{S}(t,t')$ is the relative second-order orientation tensor and the normalization factor 15/4 in Eq. (2) is replaced by $15/3 = 5$ to recover the shear modulus at small strains. Figure 1 shows a schematic illustration of the independent alignment assumption (IAA) where stress after rapid equilibration of chain stretch is created by affine rotation of tube segments [7]. The linear-viscoelastic relaxation modulus

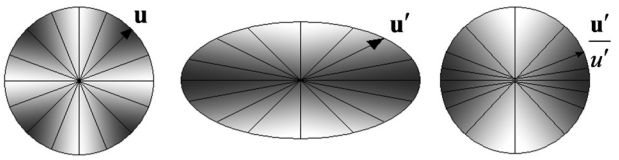

FIG. 1. Schematic illustration of the independent alignment assumption (IAA) of DE theory, i.e. the stress tensor after equilibration of chain stretch is the result of a mere change in chain orientation, sometimes called "affine rotation."

$G(t-t')$ is defined in multimode Maxwell form,

$$G(t-t') = G_N^0 F(t-t') = \sum_i g_i e^{-(t-t')/\tau_i}. \tag{6}$$

Here, the set of $\{g_i, \tau_i\}$ defines the discrete Maxwell modes, G_N^0 is the plateau modulus derived from the rubber elasticity theory [8,9], and function $F(t-t')$ is related to the survival probability of a tube segment for the time interval $(t-t')$ of the strain history [4,10].

The deformation tensors $\mathbf{S}_{\mathbf{DE}}$ and $\mathbf{S}_{\mathrm{DE}}^{\mathrm{IA}}$ both lead to similar results in the case of elongational flow; yet, they lead to different predictions of the second normal stress difference, and consequently, also of biaxial extensional flows [11]. It should be noted that if the relaxation modulus is expressed as the sum of Maxwell modes, the DE model is basically a multimode equation obeying time-deformation separability, i.e. with a "universal" deformation tensor independent of molecular weight and molecular weight distribution. The DE model, in its original form, has shown several insufficiencies in modeling the linear and nonlinear viscoelastic properties of polymers, and therefore, several modifications have been made to this model. In the linear-viscoelastic regime (LVE), contour length fluctuations (CLF) [12] and constraint release (CR) [13] were introduced to the DE model to address the experimentally observed disagreements between the LVE behaviors of linear entangled polymers and the DE theory. In the nonlinear viscoelastic regime, the predictions of the DE model are only in qualitative agreement with the flow behavior of monodisperse linear entangled melts subjected to shear deformation whereas the model does not predict the strain hardening in the start-up of the extensional flows [14]. These have led to the introduction of convective constraint release (CCR) [15] (to avoid the excessive shear thinning) as well as chain stretch mechanisms [2,16] to the nonlinear viscoelastic regime of the DE model.

III. TUBE-BASED MODELS WITH PREAVERAGED CHAIN STRETCH

In order to resolve the mentioned inconsistencies between the DE model and the start-up of extensional flows, a stretch mechanism for the polymer chain was incorporated into the original model [2]. With $L_0 = Na_0$ being the equilibrium length of the tube, and by assuming a uniform stretch with stretch ratio λ along the contour length, $L(t) = \lambda Na_0$, the extra-stress tensor is given as

$$\boldsymbol{\sigma}(t) = \frac{G_N^0}{\bar{L}^2}\left\langle \int_0^{L(t)} dsL(t)(\mathbf{uu}) \right\rangle \approx G_N^0\lambda^2\left\langle \frac{1}{L(t)}\int_0^{L(t)} ds(\mathbf{uu}) \right\rangle = 3G_N^0\lambda^2\bar{\mathbf{S}}(t). \tag{7}$$

Here, s denotes the position of the orientation vector $\mathbf{u}$ of a chain segment at time t, $\mathbf{u} = \mathbf{u}(s, t)$, and $\bar{\mathbf{S}}(t)$ is the orientation tensor with $tr(\bar{\mathbf{S}}(t)) = 1$ describing the average orientation of chain segments at time t. The stress is a quadratic function of the preaveraged stretch ratio $\lambda(t) = L(t)/L_0$, and the pre-averaging of the stretch was DE's primary approach to correct the inconsistencies of the original model particularly at high Deborah numbers. The approximation in Eq. (7) becomes exact for step-strain deformations. For time-dependent flows, stretch and orientation are assumed to be decoupled, and the stretch $\lambda(t)$ is an explicit function of the observation time t. In the following, Eq. (7) was approximated by a single integral equation with the preaveraged stretch $\lambda(t)$ in front of the integral,

$$\boldsymbol{\sigma}(t) = 3\lambda^2(t)G_N^0\bar{\mathbf{S}}(t) = \lambda^2(t)\int_{-\infty}^{t}\frac{\partial G(t-t')}{\partial t'}\mathbf{S}_{\mathbf{DE}}(t')dt'. \quad (8)$$

Equation (8) created the need to relate stretch to deformation. Pearson *et al.* [17] developed a stretch evolution equation based on a mean-field approximation by considering the balance between the frictional force on the chain, and the spring force created in the chain,

$$\frac{\partial\lambda}{\partial t} = \lambda(\mathbf{K}:\bar{\mathbf{S}}) - \frac{1}{\tau_R}(\lambda - 1), \quad (9)$$

where $\mathbf{K}$ is the velocity gradient tensor and $\tau_R = kM^2$ is the Rouse relaxation time. The first term on the right-hand side of Eq. (9) represents the affine stretch of the chain by the drag of the surrounding chains, the second term denotes the Rouse stretch relaxation mechanism, and $(\lambda - 1)$ ensures the unity of stretch at equilibrium. Equation (9) expresses the deformation rate-dependent chain stretch by the inclusion of the stretch relaxation time τ_R in the evolution equation. We note here that Eq. (9) predicts unbounded stretch in elongational flow for $Wi_R = \dot{\varepsilon}\tau_R \to 1$ (Weissenberg number in terms of elongational rate $\dot{\varepsilon}$ and τ_R), which necessitates the consideration of finite extensibility. However, for simplicity, we will not discuss finite extensibility effects in the following.

In polydisperse polymeric systems, there are macromolecules with different molar masses and different topologies. To obtain agreement of model predictions and experimental evidence for polymers with a wide spectrum of relaxation times, it was necessary to develop multimode models with n discrete modes, where each mode is characterized by a partial relaxation modulus g_i and a relaxation time τ_i representing one virtual molecular species. Assuming a linear superposition of the nonlinear contributions of the relaxation modes, the multimode version of the extra-stress tensor then becomes [18]

$$\boldsymbol{\sigma}(t) = \sum_i^n 3g_i\lambda_i^2(t)\bar{\mathbf{S}}_i(t) = \sum_i^n g_i\mathbf{c}_i(t). \quad (10)$$

Here, $\bar{\mathbf{S}}_i$ and $\mathbf{c}_i$ signify the orientation and conformation tensors, respectively, of mode i, and the average stretch λ_i of the ith relaxation mode becomes

$$\lambda_i(t) = \sqrt{\frac{tr(\mathbf{c}_i(t))}{3}}. \quad (11)$$

Thus, even for models formulated in terms of the conformation tensors $\mathbf{c}_i$ without an explicit evolution equation for the stretch, stretch of mode i is an explicit function of observation time t [according to Eq. (11)] representing the average stretch of all molecular species of type i.

In the following, we consider multimode versions of two tube-based models, the Marrucci and Ianniruberto model [19] and the Rolie-Poly model of Likhtman and Graham [20], which have been used for the characterization of polydisperse linear polymer melts, as well as two tube-based models for LCB melts, the pom-pom model of McLeish and Larson [21] and the extended pom-pom model (XPP) model of Verbeeten *et al.* [22]. All these models are based on the concept of Eqs. (10) and (11).

A. Tube-based models for polydisperse linear polymer melts

1. Marrucci and Ianniruberto model (2003)

Following the earlier modeling works [15,23,24], Marrucci and Ianniruberto (M&I) [19] developed a differential constitutive equation in terms of the conformation tensor that includes the effect of double reptation (Tsenoglou [25], Des Cloizeaux [26], and Tsenoglou [27]) and CCR effects [15,23,24], as well as Rouse stretch relaxation for monodisperse entangled linear polymers. In this way, orientation and stretch are coupled, but stretch remains an explicit function of time t according to Eq. (11). The model was originally developed as a one-mode "toy" model for monodisperse linear melts. The multimode version of this model can be expressed as [28]

$$\overset{\nabla}{\mathbf{c}}_i = -\frac{1}{\tau_{ei}}(\mathbf{c}_i - \lambda_i^2\mathbf{I}) - \frac{1}{\tau_{\mathrm{R}i}}(\lambda_i^2 - 1)\mathbf{I}, \quad (12)$$

where $\overset{\nabla}{\mathbf{c}} = (D/Dt)\mathbf{c} - \mathbf{K}^T\cdot\mathbf{c} - \mathbf{c}\cdot\mathbf{K}$ is the upper convected derivative of the conformation tensor and λ_i is given in Eq. (11). τ_{ei} is the effective orientation time defined with reference to the reptation (disengagement) time τ_{di}, the Rouse time τ_{Ri}, and the CCR parameter β_{ccr},

$$\frac{1}{\tau_{ei}} = \frac{2}{\tau_{di}} + \left(\frac{1}{\tau_{\mathrm{R}i}} - \frac{2}{\tau_{di}}\right)\frac{\beta_{\mathrm{ccr}}(\lambda_i^2 - 1)}{1 + \beta_{\mathrm{ccr}}(\lambda_i^2 - 1)}. \quad (13)$$

Here, due to the effect of double reptation, the reptation time τ_{di} is taken as twice the relaxation time τ_i of mode i as defined by the relaxation modulus according to Eq. (6), i.e., $\tau_{di} = 2\tau_i$. In this way, thermal CR is implicitly taken into account (see, e.g., Leygue *et al.* [29]). The reducing effect of CCR on τ_{ei} becomes noticeable during fast deformations, when $\lambda_i > 1$. As shown in Eqs. (10)–(13), the M&I model requires two linear (g_i, τ_i) and one nonlinear free parameter ($\tau_{\mathrm{R}i}$) per mode of relaxation as well as the CCR free parameter β_{ccr}, which is assumed constant for the entire relaxation process.

Figure 2 shows as an example of the predictions of an 8-mode M&I model for the steady shear and the start-up elongational viscosity of a commercial grade polystyrene (Styron 648) by Boukellal *et al.* [30]. While the steady shear viscosity is captured nicely over many decades of shear rate, the agreement of time-dependent elongational viscosity data and model predictions is marginal.

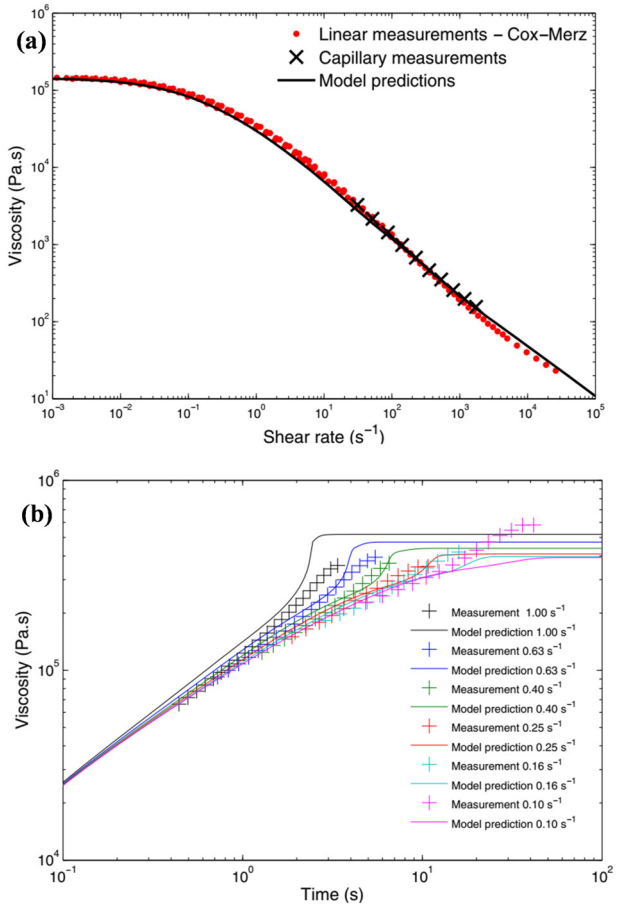

FIG. 2. The comparison between experimental and computed viscosity of PS 648 via an 8-mode M&I model: (a) steady shear behaviour and (b) elongational viscosity. Reprinted with permission from Boukellal, G., A. Durin, R. Valette, and J.-F. Agassant, "Evaluation of a tube-based constitutive equation using conventional and planar elongation flow optical rheometers," Rheol. Acta **50**, 547 (2011). Copyright 2011, Springer.

Wapperom and Keunings [31] applied the M&I model in contraction/expansion flow simulations of two nearly monodisperse polymer solutions. Furthermore, Agassant and Mackley [32] used the M&I model to fit the data of Boukellal *et al.* [30]. Recently, Varchanis *et al.* [28] compared the simulation results of 4-mode and 6-mode versions of M&I, Rolie-Poly, Phan-Thien and Tanner (PTT) [33], and Giesekus model [34] for the unsteady channel flow as well as the contraction-expansion slit flow to the experimental data. They found acceptable agreement between those models and the experimental data although the tube-based models performed better with respect to both the rheological and the inhomogeneous flow data.

2. *The Rolie-Poly model (2003)*

The single-mode version of the Rolie-Poly model of Likhtman and Graham [20] was derived as a simplified differential approximation of the Graham–Likhtman and Milner–McLeish (GLaMM) model [35] that links the CCR effect to the Rouse dynamics of the tube [28]. The Rolie-Poly model accounts for the CCR effect as well as reptation and chain retraction mechanisms. The multimode version of the Rolie-Poly model was already used by Likhtman and Graham [20] and is given as

$$\overset{\nabla}{\mathrm{c}}_i = -\frac{1}{\tau_i}(\mathrm{c}_i - \mathrm{I}) - \frac{f_{\mathrm{retr}}}{\tau_{\mathrm{R}i}}[\mathrm{c}_i + f_{\mathrm{ccr}}(\mathrm{c}_i - \mathrm{I})]. \tag{14}$$

The function f_{retr} stands for the chain retraction mechanism as a function of stretch, and its multimode form becomes

$$f_{\mathrm{retr}} = 2\left(1 - \frac{1}{\lambda_i}\right) \tag{15}$$

with λ_i defined as the explicit function of time t in Eq. (11). The CCR effect of the Rolie-Poly model is expressed by the function f_{ccr},

$$f_{\mathrm{ccr}} = \beta_{\mathrm{ccr}}\lambda_i^{2\delta}, \tag{16}$$

where β_{ccr} and δ are the fitting parameters. It is generally assumed that δ is equal to $-1/2$ [20,28]. Thus, the nonlinear free parameters of the Rolie-Poly model, Eqs. (10), (11) and (14)–(16), for each mode are $\tau_{\mathrm{R}i}$ and β_{ccr}, as in the case of the M&I model. As pointed out by Likthman and Graham, in the limit of vanishing stretch relaxation time, Eq. (14) resembles the original Marrucci CCR equation [23]. Figure 3 shows the predictions of a 9-mode Rolie-Poly model for the transient shear and elongational viscosity of a polydisperse commercial polystyrene melt (PS2) as reported by Lord *et al.* [36].

Bouadara and Read [37] used the Rolie-Poly model (with finite extensibility) to develop a simplified stochastic toy model for star polymers [38,39]. Their model showed satisfactory results in the linear regime; yet, they observed dramatic changes in the stress growth coefficient in the nonlinear regime as they navigated around the parameter map. The Rolie-Poly model was applied in several numerical simulation studies such as Valette *et al.* [40] for pressure driven flow behavior of linear low-density polyethylene melt flowing within an entry and exit slit geometry using 6 modes; Lord *et al.* [36] in 3D viscoelastic numerical simulation using a multipass rheometer for both an entry-exit slit flow and a cross-slot geometry (9 modes); and Collis *et al.* [41] for the simulation of time dependent flow of polymer in multipass rheometer (6 modes).

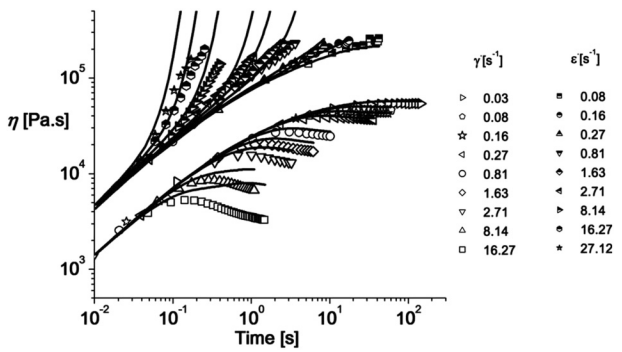

FIG. 3. Nonlinear shear and uniaxial extensional transient viscosities η data (symbols) for PS2 at a reference temperature of 180 °C with corresponding fits of a 9-mode Rolie-Poly model (solid lines). Reprinted with permission from Lord, T., L. Scelsi, D. Hassell, M. Mackley, J. Embery, D. Auhl, O. Harlen, R. Tenchev, P. Jimack, and M. Walkley, "The matching of 3D Rolie-Poly viscoelastic numerical simulations with experimental polymer melt flow within a slit and a cross-slot geometry," J. Rheol. **54**, 355–373 (2010). Copyright (2010), The Society of Rheology.

B. Tube models with preaveraged chain stretch for LCB polymers

1. The pom-pom model (1998)

The pom-pom model was developed by McLeish and Larson [21] for an idealized LCB polymer with q side chain branches attached to both ends of the backbone incorporating the concept of the preaveraged chain stretch of the DE tube model. The backbone chain with molar mass M_b is kept within the tube via the net Brownian force exerted on the free chain ends. Consequently, the maximum magnitude of chain stretch is equal to the number of dangling arms, $\lambda_{\max} = q$. Accordingly, at the onset of maximum stretch, branch point withdrawal (BPW) takes effect and the arms are drawn into the tube of the backbone.

The nonlinear response of the backbone starts when the strain rate becomes greater than the inverse of the backbone relaxation time (τ_b^{-1}) and smaller than the arm relaxation time (τ_a^{-1}), i.e., $\tau_b^{-1} < \dot{\varepsilon} < \tau_a^{-1}$. The evolution equation of the dimensionless stretch parameter of the pom-pom model is given as

$$\frac{\partial \lambda}{\partial t} = \lambda(\mathbf{K}:\bar{\mathbf{S}}) - \frac{1}{\tau_s}(\lambda - 1), \quad \text{for} \quad \lambda < q. \tag{17}$$

We note the similarity between Eqs. (17) and (9), with the Rouse time replaced by τ_s, the stretch relaxation time scaling with the number of arms (q), and the arm relaxation time τ_a. The stretch limit on the right-hand side of Eq. (17) initiates abrupt cessation of backbone stretch (shown as unphysical cusps in steady-state viscosity during uniaxial extension) at $\lambda_{\max} = q$ suggesting an unrealistic sudden retraction of arms. This inconsistency of the pom-pom model was later addressed by Blackwell *et al.* [42] based on the fact that the zero-shear viscosity (and relaxation time) of LCBs does not follow $\eta_0 = kM_w^{\alpha}$ [43], and instead, it is dependent on the arm length, i.e., $\eta_0 = (M_a/M_e)^{\beta} \exp(\upsilon M_a/M_e)$. This relation was applied to modify the stretch relaxation time in Eq. (17)

$$\frac{\partial \lambda}{\partial t} = \lambda(\mathbf{K}:\bar{\mathbf{S}}) - \frac{1}{\tau_s}(\lambda - 1)e^{\upsilon(\lambda-1)} \tag{18}$$

and was named "drag-strain coupling." The coefficient in the smoothing exponential term in Eq. (18) with values $0 < \upsilon = 2/q < 1$ allows for the gradual arm retraction as opposed to the abrupt cessation of the backbone stretch in the original pom-pom model. Inkson *et al.* [44] proposed the multimode pom-pom model to account for the multiple branching structure of industrial LCBs, which is modelled by a sequence of virtual pom-pom molecules with multiple moduli g_i and relaxation times τ_i, and a stress tensor according to Eq. (10). The orientation tensors $\bar{\mathbf{S}}_i$ are simplistically expressed as

$$\bar{\mathbf{S}}_i = \mathbf{c}_i / tr(\mathbf{c}_i) \tag{19}$$

and the conformation tensors c_i follow the differential relation of the upper convective Maxwell model

$$\overset{\nabla}{\mathbf{c}}_i = -\frac{1}{\tau_i}(\mathbf{c}_i - \mathbf{I}) \tag{20}$$

with the relaxation times τ_i as the backbone orientation times. The closed form solution of Eq. (19) was given by Rubio and Wagner [45,46] and McKinley and Hassager (Appendix B in [47]). The evolution equations of stretch in the multimode pom-pom model are obtained by generalizing Eq. (18) [44],

$$\frac{\partial \lambda_i}{\partial t} = \lambda_i(\mathbf{K}:\bar{\mathbf{S}}) - \frac{1}{\tau_{si}}(\lambda_i - 1)e^{\upsilon_i(\lambda_i - 1)} \quad \text{with} \quad \upsilon_i = 2/q_i. \tag{21}$$

The number of arms q_i and the backbone stretch relaxation time τ_{si} are the nonlinear fitting parameters of each mode in multimode pom-pom model.

Figure 4 demonstrates the predictions of a 9-mode pom-pom model for transient shear and elongational viscosity of IUPAC A low-density polyethylene (LDPE) [44].

The pom-pom model was utilized, e.g. in the numerical simulation studies of Bishko *et al.* [49] for transient flow of branched polymer melts through a planar contraction; Wapperom and Keunings [50] for describing linear polymer melts; Sirakov *et al.* [51] for analyzing the viscoelastic flow of branched LDPE through 3D planar contraction geometry (9 modes); and Vittorias *et al.* [52] in the simulation of the industrial polyethylene of various molecular weight distributions using a 4-mode differential pom-pom model.

2. The extended pom-pom model (2001)

Verbeeten *et al.* [22] proposed the XPP by incorporation of the anisotropic drag idea of Giesekus [34] to address the limitations of the pom-pom model: (i) lack of predictions of the second normal stress difference [45–47], (ii) unboundedness

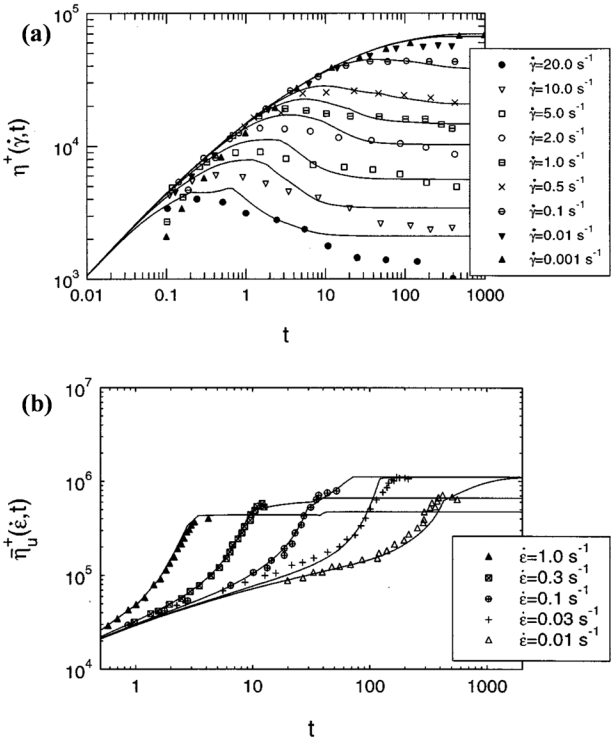

FIG. 4. The predictions of a 9-mode pom-pom model for (a) transient shear viscosity, (b) transient uniaxial extensional viscosity of IUPAC A LDPE melt data of [48]. Reprinted with permission from Inkson, N. J., T. G. B. McLeish, O. G. Harlen, and D. J. Groves, "Predicting low density polyethylene melt rheology in elongational and shear flows with pom-pom constitutive equations," J. Rheol. **43**, 873–896 (1999). Copyright (1999), The Society of Rheology.

of the equation of orientation at high strain rates, and (iii) discontinuity of the steady-state uniaxial extensional viscosity of solutions [53]. In addition to the two nonlinear parameters per mode of the multimode pom-pom model, the XPP model added a Giesekus (anisotropic) parameter α_i to predict the non-zero second normal stress coefficient ψ_2, and thus the evolution equation of the conformation tensors $\mathbf{c}_i$ is formulated as

$$\overset{\nabla}{\mathbf{c}}_i = -\alpha_i(\mathbf{c}_i - \mathbf{I})^2 - F_{XPP}\mathbf{c}_i - \mathbf{I}. \tag{22}$$

Here, F_{XPP} is the extra function of the XPP model, which takes into account the orientational relaxation (τ_i), and the stretch relaxation (τ_{si}) depending on the number of virtual chain arms (q_i)

$$F_{XPP} = 2\frac{\tau_i}{\tau_{si}}\left[\frac{2}{q_i}(\lambda_i - 1)\right]\left(1 - \frac{1}{\lambda_i}\right) + \frac{1}{\lambda_i^2}\left[1 - \alpha_i - \frac{\alpha_i}{3}tr(\mathbf{c}_i^2 - 2\mathbf{c}_i)\right] \tag{23}$$

with λ_i as defined in Eq. (11). The stress tensor of the XPP model is given by Eq. (10). The Giesekus model is recovered when $F_{XPP} = 1$, and $\alpha_i = 0$ leads to the simplified version of the XPP model [53]

$$\overset{\nabla}{\mathbf{c}}_i = F_{XPP}\mathbf{c}_i - \mathbf{I} \tag{24}$$

with

$$F_{XPP} = 2\frac{\tau_i}{\tau_{si}}\exp\left[\frac{2}{q_i}(\lambda_i - 1)\right]\left(1 - \frac{1}{\lambda_i}\right) + \frac{1}{\lambda_i^2}. \tag{25}$$

Figure 5 shows the XPP model predictions of the transient and steady state (insets) of elongational viscosity, shear viscosity, and first normal stress coefficient ψ_1 of Lupolen 1810H LDPE melt with 6 relaxation modes [22].

Tanner and Nasseri [54] considered the XPP, Giesekus, and PTT model in the framework of a general network model and discussed the ability of single and multimode versions to fit elongation, shear, planar, and biaxial extension data of linear and branched polymers. Pivokonsky *et al.* discussed the fitting capabilities of multimode versions of the XPP, PPT, and a modified Leonov model [55,56] for branched [57] and linear polyethylene melts [58]. Pivokonsky *et al.* [59] used a 6-mode versions of the XPP and PTT model to characterize linear and branched polypropylene melts. Pivokonsky and Filip [53] showed that the three nonlinear parameters per mode of the XPP model can be reduced to two parameters and still result in comparable fitting quality for the shear and elongational rheology of three LDPE melts with 8 to 10 modes.

Pivokonsky *et al.* [58] applied both XPP and PTT-XPP models for the quantification of branching level of metallocene catalysed polypropylene (mPP). They showed that based on the activation energy results, the processed mPP has star-branched structure, and the PTT-XPP model provides the best predictions for the rheological characterization of processed mPP. The numerical simulation applications of the XPP model are given in Verbeeten *et al.* [60] to simulate a low density polyethylene melt in a transient contraction flow (4 modes); Sirakov *et al.* [51] in viscoelastic contraction flows (9-mode); and Sarafrazi and Sharif [61] for non-isothermal flow in film

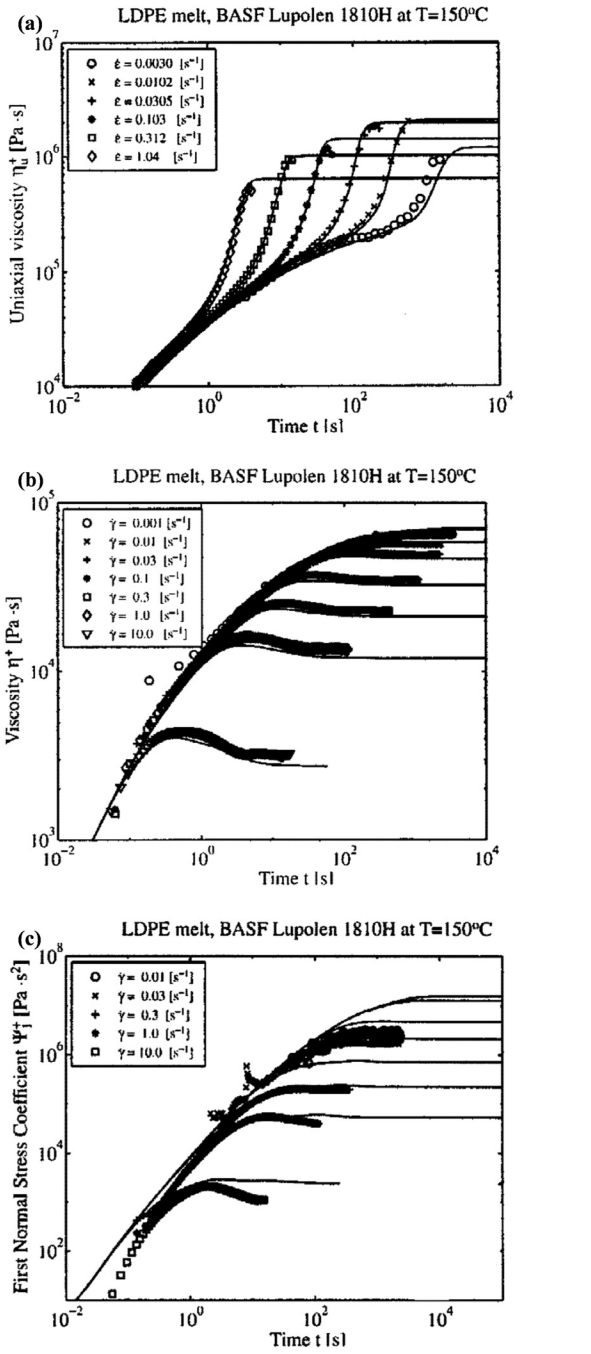

FIG. 5. (a) Transient and quasi-steady state (inset) elongational viscosity of a 6-mode XPP model for Lupolen 1810H melt at T = 150 °C. (b) Transient and steady state (inset) shear viscosity η (left) and first normal stress coefficient ψ_1 (right) of a 6-mode XPP model for Lupolen 1810H melt at T = 150 °C. Reprinted with permission from Verbeeten, W. M. H., G. W. M. Peters, and F. P. T. Baaijens, "Differential constitutive equations for polymer melts: The extended pom-pom model," J. Rheol. **45**, 823–843 (2001). Copyright (2001), The Society of Rheology.

blowing process (4 modes). Russo and Phillips [62] reported numerical prediction of the XPP model for extrudate swell of six LCB polymers (6 modes). A similar study using the 8-mode XPP and PPT models was conducted by Ganvir *et al.* [63]. Oishi *et al.* [64] reported numerical solutions of the XPP model for the viscoelastic free surface flows.

The XPP model has been criticized for generating mathematical defects [65] and unphysical (e.g., turning points,

bifurcation, multiple solution, etc.) solutions [18,66,67]. Not only is the occurrence of multiple unphysical solutions a unique characteristic of the XPP model but also it is a common aspect of nonlinear differential type rheological equations [18]. Inspired by the study of Schleiniger and Weinacht [68] on the Giesekus model, Baltussen *et al.* [18] proposed a constraint on the anisotropy parameter, i.e. $\alpha < 0.5$, to generate only one solution from the XPP model. This constraint is most restrictive in elongational flow and at high stretch when $\lambda \to q$.

C. Summary of tube-based models with preaveraged stretch

The four models which have been reviewed so far are all based on the stress tensor given in Eq. (10), and even when expressed by the conformation tensors $\mathbf{c}_i$, the average stretch of mode i is an explicit function of time as expressed by Eq. (11). The basic concept of these constitutive equations is thus the assumption of preaveraged chain stretch per mode, which goes back to the fundamental assumption of the DE model that the tube diameter is constant and independent of deformation, and consequently the chain tension is the same everywhere along the tube. Stretch is governed by the Rouse times τ_{Ri} (linear melts) or the stretch relaxation times τ_{si} (LCB melts). For LCB melts, the number of virtual arms (q_i) is an additional fitting parameter. While one-mode versions of the models are in rough qualitative agreement with experimental evidence of monodisperse melts and therefore are sometimes termed "toy models," quantitative prediction of the rheology of polydisperse linear and randomly LCB polymer melts is only possible by use of multimode models based on a set (g_i, τ_i) of discrete Maxwell modes with at least 1 (linear melts) or 2 (LCB melts) nonlinear parameters per mode, which have to be fitted to the nonlinear viscoelastic data. With typically 4–9 modes needed to describe the experimentally accessible window, this amounts to 4–9 (linear melts) or 8–18 (LCB melts) nonlinear fitting parameters, and it is difficult to confidently assign physical significance to those parameters. One may of course argue that in polydisperse linear or randomly branched polymer melts, there is a vast variety of different chain lengths and chain connectivity, and in principle each chain strand should have its own set of nonlinear parameters. Here, we should briefly acknowledge the recent efforts made to predict the large number of nonlinear parameters *a priori* from known molecular weight distributions and considering the effects of inter- and intrachain connectivity on the nonlinear rheology of polydisperse linear and LCB polymers. Mead *et al.* [69] proposed a constitutive model (MP model) for entangled polydisperse linear melts presenting a quantitative description of the entanglement dynamics manifested through the time-dependent plateau modulus. The definition of "tube" in this model is a series of discrete oriented *ij* set of entanglement pairs along the chain rather than the classic mean-field description of the tube [70]. The MP model was applied [71] to model the shear modification following the cessation of fast shear deformations of PS melt data of Tsang and Dealy [72,73]. The MP polydisperse model revealed that the high molecular weight components of molar mass distribution contribute equally to the bulk stress when low molecular weight components present a solvent-like effect. Moreover, Read *et al.* [74] developed a predictive scheme to calculate the linear and nonlinear viscoelasticity of stochastically branched polymer melt as a function of the chemical kinetics of its formation through the numerical simulation of its polymerization. They showed that by controlling the degree of branching and molecular weight, the linear and extension hardening behaviors of LDPE resin can be controlled. Recent work of Read and co-workers [75] reconsidered the Roly-Poly model in view of the double reptation approximation [26] and achieved qualitative and (to some extent) quantitative agreement with the experimental data of bidisperse and polydisperse linear melts.

These molecular based models, which are outside of the scope of this review, are certainly an improvement over the linear superposition models discussed in Sec. III, albeit at the expense of considerable complexity in the modeling assumptions made, and the numerical efforts required. However, one may also argue that the effect of polydispersity of chain length and of connectivity manifests itself already in the linear-viscoelastic relaxation modulus. By reassessment of the modeling assumptions, particularly the assumption of preaveraged chain stretch and constant tube diameter, the number of nonlinear material parameters can be reduced drastically as shown in the following.

IV. TUBE MODELS WITHOUT PREAVERAGED CHAIN STRETCH FOR POLYDISPERSE POLYMER MELTS

A. The MSF model (2003)

The molecular stress function (MSF) model, developed over the years by Wagner and Schaeffer [76–78], Wagner *et al.* [79], and Wagner *et al.* [80], is based on the strain-dependent tube diameter theory which was originally suggested by Marrucci and de Cindio [81]. The principal distinction between the MSF model and the previously discussed tube-based models is the dismissal of the preaveraged chain stretch proposed by Doi and Edwards [2], and consequently, the proposal of a strain-dependent tube diameter. The MSF model considers a tube segment containing N_e Kuhn steps of length b, which is created by reptation at time t' with diameter a_0 and length a_0. Due to deformation, at observation time t when the stress is measured, the squeezing effect of the surrounding topological constraints has reduced the tube segment diameter from a_0 to a and has stretched the tube segment by a factor f from a_0 to $l = fa_0$. According to Doi and Edwards [see Eq. (A9) in [3]], the line density n/l, i.e. the number n of monomer units of length b that are found per length l of the tube, is a well-defined thermodynamic quantity and is given by

$$\frac{n}{l} = \frac{a}{b^2}. \tag{26}$$

Thus, for a tube segment with $n = N_e$ Kuhn steps, tube diameter and stretch are related by [82]

$$N_e b^2 = a_0^2 = al = afa_0. \tag{27}$$

For Gaussian chains, stretch and tension are proportional to each other, and f was called the MSF. From relation (27) follows that $f = f(t, t')$ is the inverse of the relative tube diameter,

$$f(t, t') = a_0/a(t, t'). \tag{28}$$

Thus, it is a function of both the observation time t and the time t' of creation of tube segments by reptation with the starting condition $f(t = t', t') = 1$. During deformation, chain segments with long relaxation times, i.e. those preferably in the middle of the tube, are exposed to higher stretches $f = f(t, t')$ than chain segments with short relaxation times, i.e. those at the chain ends. According to the MSF model, stretch is considered to be a relative quantity (i.e. a quantity depending on times t and t') in the same way as the strain tensor. This is fundamentally different from the models with preaveraged stretch presented above, where stretch is an explicit function of observation time t, and stretch and tube diameter are unrelated, i.e. when chains of mode i are stretched, their tube diameter remains constant. We remark that such effects (i.e., that the center of the chain becomes more stretched than the chain ends) do also occur in the more advanced molecular models such as the GLaMM model [35] and the models shortly discussed in Sec. III C but require more detailed modeling with coupling of stretch between adjacent tube segments.

The extra stress is then given by a superposition integral of the form

$$\boldsymbol{\sigma}(t) = \int_{-\infty}^{t} \frac{\partial(G(t-t'))}{\partial t'} f^2 \mathbf{S}_{DE}^{IA} dt' = 5 \int_{-\infty}^{t} \frac{\partial(G(t-t'))}{\partial t'} f^2 \mathbf{S} dt' \tag{29}$$

with $\mathbf{S}(t, t')$ given by Eq. (5). Considering the change of free energy of backbone chain segments due to stretch and irreversible energy dissipation by a CR process, the evolution equation for f was found to be [80]

$$\frac{\partial f}{\partial t} = \frac{1}{2} \frac{\beta f}{1 + ((\beta - 1)/f^4)} \left[(\mathbf{K}:\mathbf{S}) - \frac{CR}{f^2 - 1} \right]. \tag{30}$$

The parameter β determines the slope of the elongational viscosity after the onset of strain hardening and takes the value of 1 for linear polydisperse polymers and has typically a value of 2 for LCB polymers. For comb-shaped polystyrene melts with different numbers and lengths of grafted side-chains, it could be shown that β represents the ratio of the total molar mass to backbone molar mass of the combs [83]. In the MSF model, CR means that the topological constraints (squeezing the tube with increasing deformation and therefore leading to chain stretch) are removed by convection, such that a minimum tube diameter is reached at sufficiently large deformations (extensional flows) or even a return of the tube diameter to its equilibrium dimension at large shear strains [79]. Thus, in the MSF model, CR is taken only to affect chain stretch and tube diameter. In contrast, in the models of Sec. III (e.g., in the original formulation by Marrucci [15]), CCR is taken primarily to be a mechanism for relaxing tube orientation. However, there are some recent models, by Marrucci and Ianniruberto [84], by Mead [69] (for linear chains), and by Hawke [85] (branched chains) which additionally consider changes in tube diameter due to entanglement stripping, and this is perhaps closer to the MSF picture of CR. In the MSF model, CR is considered to be the consequence of different convection mechanisms for tube orientation and tube-cross section, and for constant strain-rate flows, it can be expressed as [79]

$$CR = (f^2 - 1)^2 [a_1 CR_1 + a_2 CR_2] \tag{31}$$

with

$$CR_1 = \frac{1}{2} \sqrt{\mathbf{A}_1^2:\mathbf{S}} = \sqrt{\mathbf{D}^2:\mathbf{S}} \tag{32}$$

and

$$CR_2 = \frac{1}{2} \sqrt{|\mathbf{A}_2:\mathbf{S} - \mathbf{A}_1^2:\mathbf{S}|} = \sqrt{|\mathbf{W} \cdot \mathbf{D}:\mathbf{S}|}, \tag{33}$$

where $\mathbf{A}_1^2 = 4\mathbf{D}^2$ and $\mathbf{A}_2 = (\partial \mathbf{A}_1/\partial t) + \mathbf{A}_1^2 + 2(\mathbf{W} \cdot \mathbf{D} + \mathbf{D} \cdot \mathbf{W}^T)$ are the second-order Rivlin-Ericksen tensors and $\mathbf{D} = (1/2)(\mathbf{K} + \mathbf{K}^T)$ and $\mathbf{W} = (1/2)(\mathbf{K} - \mathbf{K}^T)$ are the rate of deformation and rotation tensor, respectively. The nonlinear material parameters verify $a_1 \geq 0$ and $a_2 \geq 0$. In extensional flows, $\mathbf{W} = 0$, and CR depends on the constraint release term CR_1 and the parameter a_1 only. At large strains, $\partial f/\partial t = 0$ and a maximum $f^2 = f_{MAX}^2$ is reached. Hence, the parameter a_1 can be expressed in terms of f_{MAX}^2 as

$$a_1 = \frac{1}{f_{MAX}^2 - 1}. \tag{34}$$

In the case of irrotational flows, the MSF model, Eqs. (29)–(34), features only two nonlinear parameters, β and $f_{\max}$, which were sufficient to model accurately the start-up and steady-state extensional viscosity of a wide variety of polydisperse linear and LCB polymers, while due to the rotational component of shear flows, the constraint release term CR_2 with the parameter a_2 is also needed. For more details, see the review by Rolón-Garrido [86]. However, it should be noted that the constraint release term CR of the MSF model is proportional to the deformation rate, and therefore after cessation of flow, there is no stretch relaxation, and the stress relaxes only by reptation. Also, the MSF model is unable to describe the elongational viscosity of monodisperse linear polymers.

Rasmussen and co-workers employed various versions of the MSF model for the numerical simulation of 3D modeling of dual wind-up extensional rheometers [87]; nano-imprint lithography [88]; Lagrangian viscoelastic flow computation [89]; isothermal compression molding to replicate the surface microstructures [90]; gas displacement of polymer melts in a cylinder [91]; and the bursting of linear polymers in inflation processes [92]. Moreover, Olley [93] and Olley and Wagner [94] used the MSF model in numerical simulations of contraction flow, and Wapperom *et al.* [95] applied the MSF model in the simulation of the large amplitude oscillatory shear of a high-density polyethylene (HDPE) melt. Recently, Wilhelm and co-workers conducted the numerical simulations using the MSF model for the uniaxial extensional flow of blends of linear and LCB polyethylene and polypropylene [96], and for the intrinsic

non-linearity of linear homopolymer melts with varying molecular weight, chemical composition, and polydispersity [97].

B. The HMMSF model (2015)

The general guidelines in the development of the Hierarchical MultiMode Molecular Stress Function (HMMSF) model have been (i) to implement Rouse stretch relaxation and the interchain tube pressure effect (Marrucci and Ianniruberto [98]), which were found to be of fundamental importance in the rheology of monodisperse linear polymer melts [14] and (ii) to recognize that the rheological effects of polydispersity and (in the case of LCB polymers) often unknown molecular structures are already contained in the linear viscoelasticity of the polymer melt. A fundamental aspect influencing the spectrum of relaxation times is "dynamic dilution" (Ball and McLeish [99]) or "tube enlargement" (Marrucci [100]), i.e. molecular structures such as segments closer to chain ends and side arms with shorter relaxation times dilute more centrally located chain segments or backbones with longer relaxation times, thereby increasing their tube diameter a. Thus, an ensemble of polydisperse linear polymer chains can be subdivided into a virtual series of chain segments characterized by relaxation times $\tau_1 < \tau_2 < \cdots < \tau_n$, which on the time scale of relaxation time τ_i, have hierarchically increasing tube diameters $a_i > a_{i-1}$. Likewise, an ensemble of LCB molecules can be thought of as a virtual series of pom-poms with hierarchically increasing relaxation times $\tau_i > \tau_{i-1}$ and backbone tube diameters $a_i > a_{i-1}$ [101] (Fig. 6). The importance of dynamic dilution for nonlinear viscoelasticity originates from the fact that it is a time-dependent process. With increasing deformation rate, there is less and less time for dynamic dilution to take place, and the full stress contribution (i.e. without the effect of dynamic dilution) of entanglements characterized by shorter and shorter relaxation times τ_i reappears in the nonlinear viscoelastic regime.

For *monodisperse* polymer melts, dynamic dilution starts from the plateau modulus G_N^0 [102]. However, for *polydisperse* polymers, there exist two dilution regimes during the relaxation process: The regime of permanent dilution, which is caused by oligomeric chains and un-entangled (fluctuating) chain ends and the regime of dynamic dilution, which begins at relaxation time $t = \tau_D$, when the relaxation process has reached the dilution modulus $G_D \le G_N^0$ (Fig. 7). The dilution modulus G_D is a free parameter of the model and is fitted to nonlinear viscoelastic data, since the mass fraction of oligomeric chains and un-entangled chain ends is in general not known *a priori*. For polydisperse linear melts, it may be expected that G_D is related to the molecular weight distribution, but a correlation has not yet been established.

If the relaxation modulus $G(t)$ of the polymer melt is represented by a sum of discrete Maxwell modes with partial relaxation moduli g_i and relaxation times τ_i,

$$G(t) = \sum_{i=1}^{n} G_i(t) = \sum_{i=1}^{n} g_i \exp(-t/\tau_i), \tag{35}$$

the square of the mass fraction w_i of dynamically diluted linear or LCB polymer segments with relaxation time $\tau_i > \tau_D$ can be determined as the ratio of the relaxation modulus at time $t = \tau_i$ to the dilution modulus $G_D = G(t = \tau_D)$, while segments with $\tau_i < \tau_D$ are considered to be permanently diluted, i.e. their weight fractions are fixed at $w_i = 1$,

$$\begin{aligned} w_i^2 &= \frac{G(t=\tau_i)}{G_D} = \frac{1}{G_D}\sum_{j=1}^{n} g_j \exp(-\tau_i/\tau_j) \quad \text{for } \tau_i > \tau_D, \\ w_i^2 &= 1 \qquad\qquad\qquad\qquad\qquad\quad \text{for } \tau_i \le \tau_D. \end{aligned} \tag{36}$$

w_D in Fig. 7 denotes the fraction of permanently diluted polymer segments,

$$w_D^2 = \frac{G(t=\tau_D)}{G_N^0} = \frac{G_D}{G_N^0}. \tag{37}$$

Accordingly, the weight fraction quantifying the total dilution (sum of permanent and dynamic dilutions) at $t = \tau_i$ (w_{Ni}^2 in Fig. 7) becomes

$$w_{Ni}^2 = \frac{G(t=\tau_i)}{G_N^0} = \frac{1}{G_N^0}\sum_{j} g_j \exp(-\tau_i/\tau_j). \tag{38}$$

The evolution equation for the MSF f_i of each mode i is

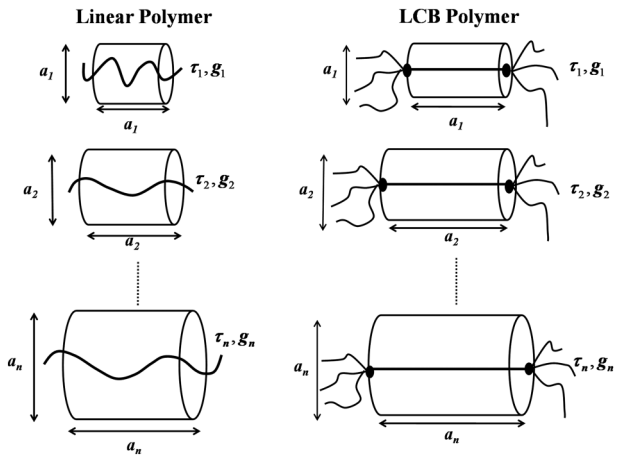

FIG. 6. Schematic illustration of the subdivision of an ensemble of polydisperse linear polymer chains into a series of hierarchically increasing tube diameter segments (left), and an LCB polymer by a hierarchical series of pom-pom polymers characterized by increasing relaxation times (right), i.e., $\tau_n > \tau_{n-i}$ and $a_n > a_{n-i}$.

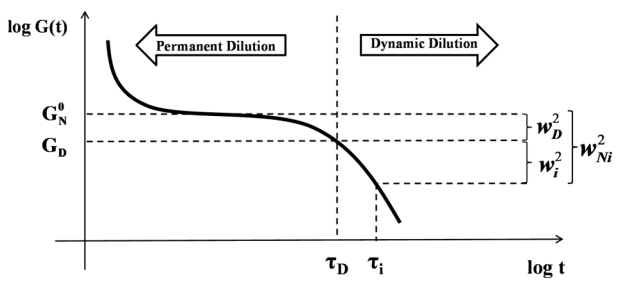

FIG. 7. Relaxation modulus and dilution dependent weight fractions of a chain segment with relaxation time τ_i in view of the permanent and dynamic dilution mechanisms of the HMMSF model. Reprinted with permission from Narimissa, E., and M. H. Wagner, "A hierarchical multi-mode molecular stress function model for linear polymer melts in extensional flows," J. Rheol. **60**, 625–636 (2016). Copyright (2016), The Society of Rheology.

expressed as

$$\frac{\partial f_i}{\partial t} = f_i(\mathbf{K}{:}\mathbf{S}) - \frac{1}{\tau_{iCR}}\left[(f_i - 1)\left(1 - \frac{2}{3}w_i^2\right) + \frac{2}{9}f_i^2(f_i^3 - 1)w_i^2\right]. \tag{39}$$

Here, the first term on the right-hand side expresses on-average affine deformation, the first term in the square bracket accounts for Rouse relaxation in the longitudinal direction of the tube, and the second term restricts the molecular stretch due to the interchain tube pressure in the lateral direction [14]. The interchain tube pressure term is proportional to w_i^2, which increases the maximum stretch of the dynamically diluted chain segments by a factor w_i, hence, erases the effect of dynamic dilution [102]. The stretch relaxation times τ_{iCR} are given by [15,103]

$$\frac{1}{\tau_{iCR}} = \frac{1}{\alpha\tau_i} + \beta_{ccr}CR_2. \tag{40}$$

The topological parameter α depends on the topology of the melt,

$$\begin{aligned} &\alpha = 1, && \text{for LCB melts,} \\ &\alpha = 1/3, && \text{for polydisperse linear melts.} \end{aligned} \tag{41}$$

In extensional flows, the stretch relaxation times for LCB melts are equal to the relaxation times of the backbone, i.e. stretch between two branch points relaxes in the same way as backbone orientation relaxes due to dynamic dilution and reptation. For broadly distributed linear polymer melts, the effective stretch relaxation time is one third of the relaxation time τ_i. As explained in [102], this is basically a consequence of the relation $\tau_i = 3Z_i\tau_{Ri}$ [2] and the fact that at $t = \tau_i$, the number of entanglements (Z) has been reduced by dynamic dilution to $Z_i \approx 1$. CR_2 denotes the dissipative CR term of Eq. (33) in rotational flows (which is zero in extensional flows), and β_{ccr} is the numerical coefficient of the CR mechanism considered as a fitting parameter in shear flow. The extra stress is given as a sum over all relaxation modes,

$$\sigma(t) = \sum_i \int_{-\infty}^{t} \frac{g_i}{\tau_i} e^{-(t-t')/\tau_i} f_i^2(t, t')\mathbf{S}_{DE}^{IA}(t, t')dt'. \tag{42}$$

Equations (36)–(42) are the main equations of the HMMSF model for the prediction of the extensional and shear flow behaviors of the linear and LCB polymer melts (differentiated by the topological parameter α). G_D is the only nonlinear free parameter of the HMMSF model in extensional flow and in conjunction with the linear-viscoelastic relaxation spectrum, it determines the degree of the strain hardening of polymer melts.

Since the molar mass distribution and the fraction of oligomeric chains and un-entangled chain ends are typically unidentified in polydisperse polymer systems, the dilution modulus remains a free parameter. As an example, Fig. 8 compares predictions of the HMMSF model with experimental data of a LDPE polymer melt (LDPE I) in uniaxial, biaxial, and planar extensional start-up flows. In the case of shear flow, an additional CR parameter β_{ccr} is needed to obtain agreement with measurements of start-up shear viscosity and first normal stress function as shown in Fig. 9 for the same LDPE melt. It should be noted that model predictions are largely independent of the number of Maxwell modes used, as shown in [101] where spectra with 7 and 17 modes gave identical results for LDPE I. While for mono- and bidisperse melts, dynamic dilution starts from the plateau modulus ($G_D = G_N^0$), the dilution modulus G_D for polydisperse melts is much lower than the plateau modulus indicating significant permanent dilution. As reported in [102,104], for polydisperse linear polymers G_D seems to be correlated with the polydispersity of the melts (as expected) and may

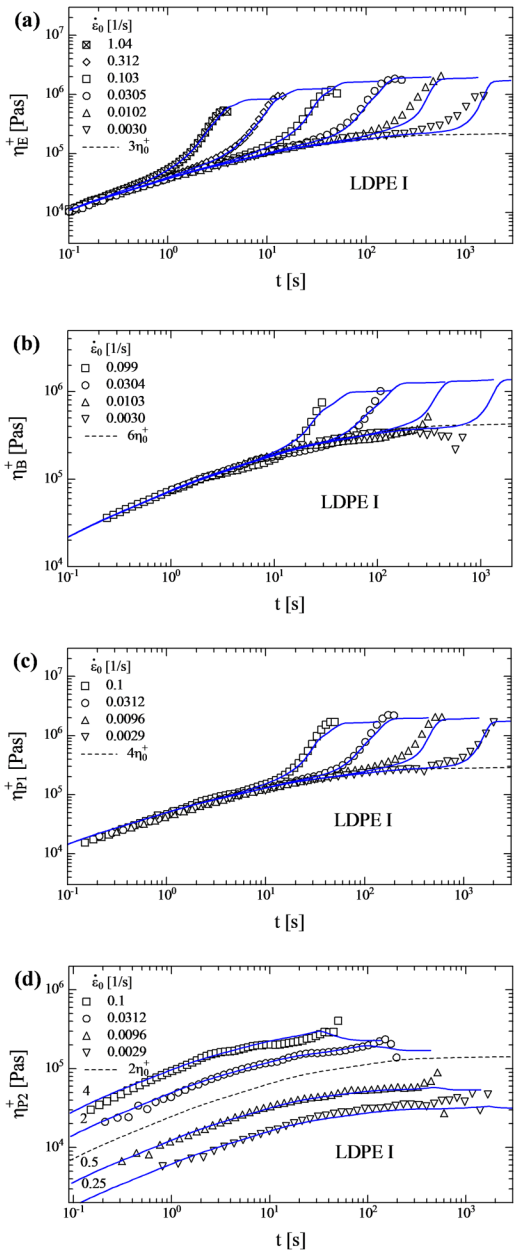

FIG. 8. Comparison of (a) uniaxial, (b) equibiaxial, as well as [(c) and (d)] first and second planar viscosity data (symbols) of LDPE I (Lupolen 1810H) melt at 150 °C with predictions of the HMMSF model (continuous lines) for a dilution modulus of $G_D = 1.5\text{E}+4$ Pa. Dotted line indicates the linear-viscoelastic start-up viscosities. Data and lines in (d) are shifted by factors 4, 2, 0.5, and 0.25 vertically. Reprinted by permission from Narimissa, E., V. H. Rolón-Garrido, and M. H. Wagner, "A hierarchical multi-mode MSF model for long-chain branched polymer melts part II: Multiaxial extensional flows," Rheol. Acta **55**, 327–333 (2016). Copyright 2016, Springer.

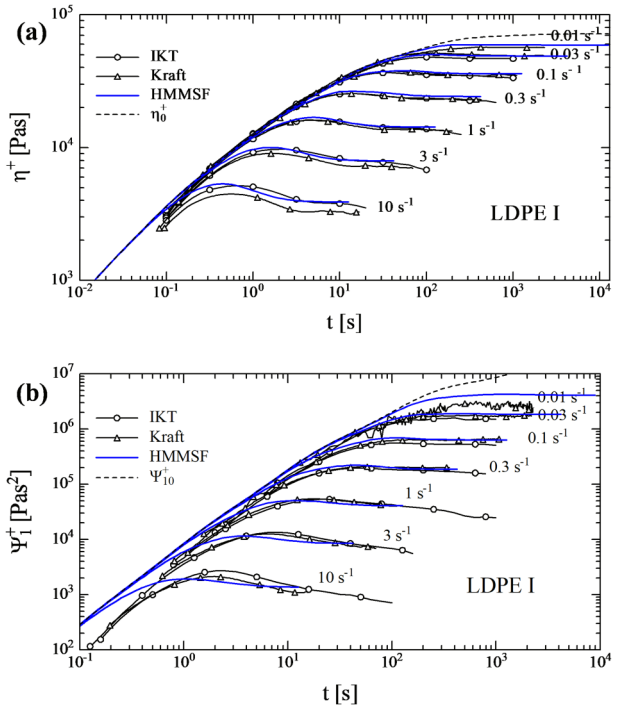

FIG. 9. Comparison of the predictions (lines without symbols) of the HMMSF model including the CR term with $G_D = 1.5\text{E}+4$ Pa and $\beta_{ccr} = 0.14$ for LDPE I with (a) shear viscosity and (b) first normal stress function data (lines with symbols). Data by Kraft [107] and Bastian [79,108] (IKT)] at 150 °C. Reprinted by permission from Narimissa, E., and M. H. Wagner, "A hierarchical multi-mode MSF model for long-chain branched polymer melts part III: Shear flow," Rheol. Acta **55**, 633–639 (2016). Copyright 2016, Springer.

eventually be extracted from the molar mass distribution. More examples of the excellent ability of the HMMSF model to fit the nonlinear viscoelasticity of polydisperse linear and LCB melts can be found in [104]. As shown in [104], the topological parameter $\alpha = 1/3$ in Eq. (41) is also valid for polymers with predominantly star architecture such as sparsely branched metallocene catalyzed polymers with typically less than one side branch per molecule. This is in agreement with recent findings of Ianniruberto and Marrucci [105] for asymmetric stars and pom-poms, which show similar steady-state nonlinear rheological behavior as linear polymers. We should also note that the HMMSF model with a suitable choice of the stretch relaxation times τ_{iccr} is able to describe the elongational viscosity of mono- and bidisperse polystyrene melts [102].

In recent studies conducted by Wingstrand *et al.* [109,110] on the effect of an ultra-high molecular weight tail (UHMW-tail) on controlled uniaxial extension and morphology of the quenched melt, they compared a blend of 1% UHMW polyethylene (UHMWPE; Mw = 4000 kg/mol) in a matrix of commercial HDPE with the pure matrix. The application of the HMMSF model on the uniaxial extension data of the UH-blend and the pure matrix at 140 °C and strain rates of 0.03–1 s^{-1} with a dilution modulus of $G_D = 350$ Pa resulted in excellent prediction of the extensional rheological behavior of the samples. Moreover, they [111] employed the HMMSF model in the study of uniaxial extensional flow induced crystallization (FIC) of HDPE melt and showed that through the incorporation of the "stretched network assumption" into the HMMSF model via modifying only the relaxation time spectrum (i.e. the longest modes affected by FIC were set to have a relaxation time of infinity), the influence of crystallization on the elongational flow can easily be captured.

V. A SHORT NOTE ON STRESS-OVERSHOOT IN ELONGATIONAL FLOW OF LCB MELTS

The occurrence of stress-overshoot in elongational flow (i.e. maximum viscosity at the end of strain hardening and prior to the steady state) of a LDPE melt was first reported by Raible *et al.* [112] and was modelled by Wagner *et al.* [113] with a generalized frame-indifferent damping function approach [114]. Yet, the earlier measurements of Laun and Münstedt [115] with a similar Meissner-type elongational rheometer did not revealed a maximum in the elongational viscosity at Hencky strains up to 6 for LDPE melt IUPAC A. Stress-overshoot in elongational flow of LCB melts has since been seen only in filament stretching rheometer (FSR) measurements by Bach *et al.* [116], Rasmussen *et al.* [117], Nielsen *et al.* [118], Huang *et al.* [119], Alvarez *et al.* [120], Hoyle *et al.* [121], and Huang [122]. Recently, Huang *et al.* [123] investigated three commercial LDPEs with two different FSRs and found elongational stress-overshoots for two LDPEs, while the third LDPE (featuring a similar strain-hardening behavior as the other two) did not show any stress-overshoot at the investigated elongation rates.

According to Burghelea *et al.* [124], the observation of maxima in elongational flow is the result of non-uniformity of sample deformation at high strains as opposed to being the material property of the polymer. Recently, Rasmussen and Fasano [125] confirmed through simulations that small variations of the sample diameter at the start of a filament stretching experiment can explain the observations of Burghelea *et al.* [124].

None of the tube-based constitutive equations discussed so far in this review can predict stress-overshoot in elongational flow. Wagner and Rolón-Garrido [126] explained the maximum in transient extensional viscosity as the disentanglement of the dangling arms after the BPW and the reversion of the LCB behavior to the linear behavior. They quantitatively modelled this phenomenon via the MSF model considering dynamic dilution, finite extensibility, stretch relaxation, and BPW mechanisms. Hoyle *et al.* [121] modified the pom-pom model to account for an additional orientation-dependent stretch relaxation process by using a relaxation rate in the stretch equation. Masubuchi *et al.* [127] used primitive slip-link simulations to model the overshoot. Hawke *et al.* [85] explained the stress-overshoot in the context of the backbone-backbone entanglement stripping due to the chain retraction in fast flows. They modified the multimode pom-pom model with a dynamic variable to account for the effect of entanglement stripping of an industrial LDPE resin. Their approach added two additional nonlinear fitting parameters (i.e., 4 in total) for each relaxation mode of a 15-mode pom-pom model and confirmed the direct relation between the degree of branching (as opposed to polydispersity) and the intensity of the stress-overshoot.

In summary, the phenomenon of stress-overshoot in elongational flow of LCB polymers with significant scientific as well as industrial interest requires further investigation of well characterized polymers and poses exciting challenges in rheological modeling.

VI. CONCLUSIONS

Multimode constitutive equations based on the assumption of preaveraged chain stretch require at least 1 (linear melts) or 2 (LCB melts) nonlinear parameters per mode, which must be fitted to nonlinear viscoelastic data. For quantitative modeling of the rheological behaviors of polydisperse linear and LCB polymer melts, a large number of nonlinear parameters are therefore required. While models of this type, especially when expressed in the form of differential equations, may still be useful for the simulation of polymer processing operations (see, e.g., Tanner and Nasseri [54]; Varchanis *et al*. [28]), they are totally inadequate for elucidating the underlying physical phenomena, and thus, for material characterization or data reduction as they do not allow reducing the complex rheological behavior of polydisperse linear and LCB polymers to a unique and limited set of material parameters.

The concept of preaveraged chain stretch goes back to the fundamental assumption of the DE model that the tube diameter is constant and independent of deformation, and consequently the chain tension is the same everywhere along the tube. Relaxing the assumption of a constant tube diameter, and relating stretch to a strain-dependent tube diameter according to the line-density concept of Doi and Edwards [3], Eq. (26), greatly reduces the number of nonlinear viscoelastic parameters needed to adequately model the rheology of linear and LCB polymers on a mesoscopic level. Additionally, taking into account the concepts of dynamic dilution through hierarchical relaxation (Ball and McLeish [99]; Marrucci [100]) and the interchain tube pressure effect (Marrucci and Ianniruberto [98]) leads to the HMMSF model, which requires only one parameter (the dilution modulus G_D) for modeling extensional flows and one additional parameter for accounting CR in shear flows, independent of the number of Maxwell modes used to define linear viscoelasticity. From the experience gained so far in modeling elongational viscosities of polydisperse linear polymer melts [102,104], it seems that G_D is indeed correlated with the polydispersity of the melts (as expected) and for linear melts may eventually be extracted from the molar mass distribution. A more challenging task will be to relate the CR parameter β_{ccr} (which has been a parameter of significant importance especially for shear flows in all tube-based models considered here) to molecular properties.

REFERENCES

[1] Dealy, J. M., D. J. Read, and R. G. Larson, *Structure and Rheology of Molten Polymers: From Structure to Flow Behavior and Back Again* (Carl Hanser Verlag GmbH Co KG, München, 2018).

[2] Doi, M., and S. F. Edwards, *The Theory of Polymer Dynamics* (Oxford University, Oxford, 1986).

[3] Doi, M., and S. F. Edwards, "Dynamics of concentrated polymer systems. Part 2—Molecular motion under flow," J. Chem. Soc. Faraday Trans. 2: Mol. Chem. Phys. **74**, 1802–1817 (1978).

[4] Doi, M., and S. F. Edwards, "Dynamics of concentrated polymer systems. Part 3—The constitutive equation," J. Chem. Soc. Faraday Trans. 2: Mol. Chem. Phys. **74**, 1818–1832 (1978).

[5] Doi, M., and S. F. Edwards, "Dynamics of concentrated polymer systems. Part 4—Rheological properties," J. Chem. Soc. Faraday Trans. 2: Mol. Chem. Phys. **75**, 38–54 (1979).

[6] De Gennes, P. G., "Reptation of a polymer chain in the presence of fixed obstacles," J. Chem. Phys. **55**, 572–579 (1971).

[7] Kheirandish, S., *Constitutive Equations for Linear and Long-Chain-Branched Polymer Melts* (Universitätsverlag der TU Berlin, Berlin, 2006).

[8] Treloar, L. R. G., "The elasticity and related properties of rubbers," Rep. Prog. Phys. **36**, 755–826 (1973).

[9] Treloar, L. R. G., *The Physics of Rubber Elasticity* (Clarendon, Oxford, 1975).

[10] De Gennes, P. G., *Scaling Concepts in Polymer Physics* (Cornell University, Ithaca, 1979).

[11] Wagner, M. H., "The nonlinear strain measure of polyisobutylene melt in general biaxial flow and its comparison to the Doi-Edwards model," Rheol. Acta **29**, 594–603 (1990).

[12] Doi, M., "Explanation for the 3.4 power law of viscosity of polymeric liquids on the basis of the tube model," J. Poly. Sci. Polym. Lett. Ed. **19**, 265–273 (1981).

[13] Daoud, M., and P. De Gennes, "Some remarks on the dynamics of polymer melts," J. Poly. Sci. Polym. Phys. Ed. **17**, 1971–1981 (1979).

[14] Wagner, M. H., S. Kheirandish, and O. Hassager, "Quantitative prediction of transient and steady-state elongational viscosity of nearly monodisperse polystyrene melts," J. Rheol. **49**, 1317–1327 (2005).

[15] Ianniruberto, G., and G. Marrucci, "On compatibility of the Cox-Merz rule with the model of Doi and Edwards," J. Non-Newton. Fluid Mech. **65**, 241–246 (1996).

[16] Marrucci, G., and N. Grizzuti, "Fast flows of concentrated polymers: Predictions of the tube model on chain stretching," Gazz. Chim. Ital. **118**, 179–185 (1988).

[17] Pearson, D. S., A. D. Kiss, L. J. Fetters, and M. Doi, "Flow-induced birefringence of concentrated polyisoprene solutions," J. Rheol. **33**, 517–535 (1989).

[18] Baltussen, M. G., W. M. Verbeeten, A. C. Bogaerds, M. A. Hulsen, and G. W. Peters, "Anisotropy parameter restrictions for the eXtended Pom-Pom model," J. Non-Newton. Fluid Mech. **165**, 1047–1054 (2010).

[19] Marrucci, G., and G. Ianniruberto, "Flow-induced orientation and stretching of entangled polymers," Philos. Trans. Royal Soc. Lond. A Math. Phys. Eng. Sci. **361**, 677–688 (2003).

[20] Likhtman, A. E., and R. S. Graham, "Simple constitutive equation for linear polymer melts derived from molecular theory: Rolie–Poly equation," J. Non-Newton. Fluid Mech. **114**, 1–12 (2003).

[21] McLeish, T. C. B., and R. G. Larson, "Molecular constitutive equations for a class of branched polymers: The pom-pom polymer," J. Rheol. **42**, 81–110 (1998).

[22] Verbeeten, W. M. H., G. W. M. Peters, and F. P. T. Baaijens, "Differential constitutive equations for polymer melts: The extended pom-pom model," J. Rheol. **45**, 823–843 (2001).

[23] Marrucci, G., "Dynamics of entanglements: A nonlinear model consistent with the Cox-Merz rule," J. Non-Newton. Fluid Mech. **62**, 279–289 (1996).

[24] Marrucci, G., "Relaxation by reptation and tube enlargement: A model for polydisperse polymers," J. Polym. Sci. Polym. Phys. **23**, 159–177 (1985).
[25] Tsenoglou, C., "Viscoelasticity of binary homopolymer blends," Polym. Prepr. Am. Chem. Soc. Div. Polym. Chem. **28**, 185–186 (1987).
[26] Des Cloizeaux, J., "Double reptation vs. simple reptation in polymer melts," Europhys. Lett. **5**, 437 (1988).
[27] Tsenoglou, C., "Molecular weight polydispersity effects on the viscoelasticity of entangled linear polymers," Macromolecules **24**, 1762–1767 (1991).
[28] Varchanis, S., Y. Dimakopoulos, and J. Tsamopoulos, "Evaluation of tube models for linear entangled polymers in simple and complex flows," J. Rheol. **62**, 25–47 (2018).
[29] Leygue, A., C. Bailly, and R. Keunings, "A differential formulation of thermal constraint release for entangled linear polymers," J. Non-Newton. Fluid Mech. **128**, 23–28 (2005).
[30] Boukellal, G., A. Durin, R. Valette, and J.-F. Agassant, "Evaluation of a tube-based constitutive equation using conventional and planar elongation flow optical rheometers," Rheol. Acta **50**, 547 (2011).
[31] Wapperom, P., and R. Keunings, "Impact of decoupling approximation between stretch and orientation in rheometrical and complex flow of entangled linear polymers," J. Non-Newton. Fluid Mech. **122**, 33–43 (2004).
[32] Agassant, J.-F., and M. R. Mackley, "A personal perspective on the use of modelling simulation for polymer melt processing," Inter. Polym. Proc. **30**, 121–140 (2015).
[33] Thien, N. P., and R. I. Tanner, "A new constitutive equation derived from network theory," J. Non-Newton. Fluid Mech. **2**, 353–365 (1977).
[34] Giesekus, H., "A simple constitutive equation for polymer fluids based on the concept of deformation-dependent tensorial mobility," J. Non-Newton. Fluid Mech. **11**, 69–109 (1982).
[35] Graham, R. S., A. E. Likhtman, T. C. McLeish, and S. T. Milner, "Microscopic theory of linear, entangled polymer chains under rapid deformation including chain stretch and convective constraint release," J. Rheol. **47**, 1171–1200 (2003).
[36] Lord, T., L. Scelsi, D. Hassell, M. Mackley, J. Embery, D. Auhl, O. Harlen, R. Tenchev, P. Jimack, and M. Walkley, "The matching of 3D Rolie-Poly viscoelastic numerical simulations with experimental polymer melt flow within a slit and a cross-slot geometry," J. Rheol. **54**, 355–373 (2010).
[37] Boudara, V. A., and D. J. Read, "Stochastic and preaveraged nonlinear rheology models for entangled telechelic star polymers," J. Rheol. **61**, 339–362 (2017).
[38] Schaefgen, J. R., and P. J. Flory, "Synthesis of multichain polymers and investigation of their viscosities1," J. Am. Chem. Soc. **70**, 2709–2718 (1948).
[39] Morton, M., T. Helminiak, S. Gadkary, and F. Bueche, "Preparation and properties of monodisperse branched polystyrene," J. Poly. Sci. **57**, 471–482 (1962).
[40] Valette, R., M. R. Mackley, and G. H. F. del Castillo, "Matching time dependent pressure driven flows with a Rolie Poly numerical simulation," J. Non-Newton. Fluid Mech. **136**, 118–125 (2006).
[41] Collis, M. W., A. K. Lele, M. R. Mackley, R. S. Graham, D. J. Groves, A. E. Likhtman, T. M. Nicholson, O. G. Harlen, T. C. B. McLeish, L. R. Hutchings, C. M. Fernyhough, and R. N. Young, "Constriction flows of monodisperse linear entangled polymers: Multiscale modeling and flow visualization," J. Rheol. **49**, 501–522 (2005).
[42] Blackwell, R. J., T. C. B. McLeish, and O. G. Harlen, "Molecular drag-strain coupling in branched polymer melts," J. Rheol. **44**, 121–136 (2000).
[43] Pearson, D. S., and E. Helfand, "Viscoelastic properties of star-shaped polymers," Macromolecules **17**, 888–895 (1984).
[44] Inkson, N. J., T. G. B. McLeish, O. G. Harlen, and D. J. Groves, "Predicting low density polyethylene melt rheology in elongational and shear flows with pom-pom constitutive equations," J. Rheol. **43**, 873–896 (1999).
[45] Rubio, P., and M. H. Wagner, "Letter to the editor," J. Rheol. **43**, 1709–1710 (1999).
[46] Rubio, P., and M. H. Wagner, "LDPE melt rheology and the pom-pom model," J. Non-Newton. Fluid Mech. **92**, 245–259 (2000).
[47] McKinley, G. H., and O. Hassager, "The Considere condition and rapid stretching of linear and branched polymer melts," J. Rheol. **43**, 1195–1212 (1999).
[48] Münstedt, H., and H. M. Laun, "Elongational behaviour of a low density polyethylene melt—II. Transient behaviour in constant stretching rate and tensile creep experiments. Comparison with shear data. Temperature dependence of the elongational properties," Rheol. Acta **18**, 492–504 (1979).
[49] Bishko, G. B., O. G. Harlen, T. C. B. McLeish, and T. M. Nicholson, "Numerical simulation of the transient flow of branched polymer melts through a planar contraction using the 'pom–pom' model," J. Non-Newton. Fluid Mech. **82**, 255–273 (1999).
[50] Wapperom, P., and R. Keunings, "Numerical simulation of branched polymer melts in transient complex flow using pom–pom models," J. Non-Newton. Fluid Mech. **97**, 267–281 (2001).
[51] Sirakov, I., A. Ainser, M. Haouche, and J. Guillet, "Three-dimensional numerical simulation of viscoelastic contraction flows using the Pom–Pom differential constitutive model," J. Non-Newton. Fluid Mech. **126**, 163–173 (2005).
[52] Vittorias, I., M. Parkinson, K. Klimke, B. Debbaut, and M. Wilhelm, "Detection and quantification of industrial polyethylene branching topologies via Fourier-transform rheology, NMR and simulation using the Pom-Pom model," Rheol. Acta **46**, 321–340 (2007).
[53] Pivokonsky, R., and P. Filip, "Predictive/fitting capabilities of differential constitutive models for polymer melts—reduction of nonlinear parameters in the eXtended Pom-Pom model," Colloid Polym. Sci. **292**, 2753–2763 (2014).
[54] Tanner, R. I., and S. Nasseri, "Simple constitutive models for linear and branched polymers," J. Non-Newton. Fluid Mech. **116**, 1–17 (2003).
[55] Leonov, A. I., and A. Prokunin, *Nonlinear Phenomena in Flows of Viscoelastic Polymer Fluids* (Springer Science & Business Media, Berlin, 2012).
[56] Zatloukal, M., "Differential viscoelastic constitutive equations for polymer melts in steady shear and elongational flows," J. Non-Newton. Fluid Mech. **113**, 209–227 (2003).
[57] Pivokonsky, R., M. Zatloukal, and P. Filip, "On the predictive/fitting capabilities of the advanced differential constitutive equations for branched LDPE melts," J. Non-Newton. Fluid Mech. **135**, 58–67 (2006).
[58] Pivokonsky, R., M. Zatloukal, and P. Filip, "On the predictive/fitting capabilities of the advanced differential constitutive equations for linear polyethylene melts," J. Non-Newton. Fluid Mech. **150**, 56–64 (2008).
[59] Pivokonsky, R., M. Zatloukal, P. Filip, and C. Tzoganakis, "Rheological characterization and modeling of linear and branched metallocene polypropylenes prepared by reactive processing," J. Non-Newton. Fluid Mech. **156**, 1–6 (2009).

[60] Verbeeten, W. M., G. W. Peters, and F. P. Baaijens, "Numerical simulations of the planar contraction flow for a polyethylene melt using the XPP model," J. Non-Newton. Fluid Mech. **117**, 73–84 (2004).

[61] Sarafrazi, S., and F. Sharif, "Non-isothermal simulation of the film blowing process using multi-mode extended pom-pom model," Inter. Polym. Proc. **23**, 30–37 (2008).

[62] Russo, G., and T. N. Phillips, "Numerical prediction of extrudate swell of branched polymer melts," Rheol. Acta **49**, 657–676 (2010).

[63] Ganvir, V., B. Gautham, R. Thaokar, A. Lele, and H. Pol, "Numerical and experimental studies on extrudate swell of branched polyethylene through axisymmetric and planar dies," J. Polym. Eng. **31**, 217–221 (2011).

[64] Oishi, C. M., F. P. Martins, M. F. Tomé, J. A. Cuminato, and S. McKee, "Numerical solution of the eXtended Pom-Pom model for viscoelastic free surface flows," J. Non-Newton. Fluid Mech. **166**, 165–179 (2012).

[65] Hulsen, M. A., "A sufficient condition for a positive definite configuration tensor in differential models," J. Non-Newton. Fluid Mech. **38**, 93–100 (1990).

[66] Clemeur, N., R. P. Rutgers, and B. Debbaut, "On the evaluation of some differential formulations for the pom-pom constitutive model," Rheol. Acta **42**, 217–231 (2003).

[67] Inkson, N., and T. N. Phillips, "Unphysical phenomena associated with the extended pom-pom model in steady flow," J. Non-Newton. Fluid Mech. **145**, 92–101 (2007).

[68] Schleiniger, G., and R. Weinacht, "A remark on the Giesekus viscoelastic fluid," J. Rheol. **35**, 1157–1170 (1991).

[69] Mead, D., S. Monjezi, and J. Park, "A constitutive model for entangled polydisperse linear flexible polymers with entanglement dynamics and a configuration dependent friction coefficient. Part I: Model derivation," J. Rheol. **62**, 121–134 (2017).

[70] Everaers, R., S. K. Sukumaran, G. S. Grest, C. Svaneborg, A. Sivasubramanian, and K. Kremer, "Rheology and microscopic topology of entangled polymeric liquids," Science **303**, 823–826 (2004).

[71] Mead, D., S. Monjezi, and J. Park, "A constitutive model for entangled polydisperse linear flexible polymers with entanglement dynamics and a configuration dependent friction coefficient. Part II. Modeling "shear modification" following cessation of fast shear flows," J. Rheol. **62**, 135–147 (2017).

[72] Dealy, J., and W. K. Tsang, "Structural time dependency in the rheological behavior of molten polymers," J. Appl. Poly. Sci. **26**, 1149–1158 (1981).

[73] Tsang, W.-W., and J. Dealy, "The use of large transient deformations to evaluate rheological models for molten polymers," J. Non-Newton. Fluid Mech. **9**, 203–222 (1981).

[74] Read, D. J., D. Auhl, C. Das, J. den Doelder, M. Kapnistos, I. Vittorias, and T. C. McLeish, "Linking models of polymerization and dynamics to predict branched polymer structure and flow," Science **333**, 1871–1874 (2011).

[75] Boudara, V. A., Read, D. J., Peterson, J. D., and Leal, L. G., "Nonlinear rheology of polydisperse blends of entangled linear polymers: Rolie-Double-Poly models," J. Rheol. **63**, 71 (2019).

[76] Wagner, M. H., and J. Schaeffer, "Nonlinear strain measures for general biaxial extension of polymer melts," J. Rheol. **36**, 1–26 (1992).

[77] Wagner, M. H., and J. Schaeffer, "Rubbers and polymer melts: Universal aspects of nonlinear stress-strain relations," J. Rheol. **37**, 643–661 (1993).

[78] Wagner, M. H., and J. Schaeffer, "Assessment of nonlinear strain measures for extensional and shearing flows of polymer melts," Rheol. Acta **33**, 506–516 (1994).

[79] Wagner, M. H., P. Rubio, and H. Bastian, "The molecular stress function model for polydisperse polymer melts with dissipative convective constraint release," J. Rheol. **45**, 1387–1412 (2001).

[80] Wagner, M. H., M. Yamaguchi, and M. Takahashi, "Quantitative assessment of strain hardening of low-density polyethylene melts by the molecular stress function model," J. Rheol. **47**, 779–793 (2003).

[81] Marrucci, G., and B. de Cindio, "The stress relaxation of molten PMMA at large deformations and its theoretical interpretation," Rheol. Acta **19**, 68–75 (1980).

[82] Wagner, M. H., "Origin of the C2 term in rubber elasticity," J. Rheol. **38**, 655–679 (1994).

[83] Wagner, M. H., J. Hepperle, and H. Münstedt, "Relating rheology and molecular structure of model branched polystyrene melts by molecular stress function theory," J. Rheol. **48**, 489–503 (2004).

[84] Ianniruberto, G., and G. Marrucci, "Shear banding in Doi–Edwards fluids," J. Rheol. **61**, 93–106 (2017).

[85] Hawke, L., Q. Huang, O. Hassager, and D. J. Read, "Modifying the pom-pom model for extensional viscosity overshoots," J. Rheol. **59**, 995–1017 (2015).

[86] Rolón-Garrido, V. H., "The molecular stress function (MSF) model in rheology," Rheol. Acta **53**, 663–700 (2014).

[87] Yu, K., J. M. R. Marín, H. K. Rasmussen, and O. Hassager, "3D modeling of dual wind-up extensional rheometers," J. Non-Newton. Fluid Mech. **165**, 14–23 (2010).

[88] Marín, J. M. R., H. K. Rasmussen, and O. Hassager, "3D simulation of nano-imprint lithography," Nanoscale Res. Lett. **5**, 274 (2009).

[89] Rasmussen, H. K., "Lagrangian viscoelastic flow computations using a generalized molecular stress function model," J. Non-Newton. Fluid Mech. **106**, 107–120 (2002).

[90] Eriksson, T., and H. K. Rasmussen, "The effects of polymer melt rheology on the replication of surface microstructures in isothermal moulding," J. Non-Newton. Fluid Mech. **127**, 191–200 (2005).

[91] Rasmussen, H. K., and T. Eriksson, "Gas displacement of polymer melts in a cylinder: Experiments and viscoelastic simulations," J. Non-Newton. Fluid Mech. **143**, 1–9 (2007).

[92] Rasmussen, H. K., and A. Bach, "On the bursting of linear polymer melts in inflation processes," Rheol. Acta **44**, 435–445 (2005).

[93] Olley, P., "A study of the quadratic molecular stress function constitutive model in simulation," J. Non-Newton. Fluid Mech. **125**, 171–183 (2004).

[94] Olley, P., and M. Wagner, "A modification of the convective constraint release mechanism in the molecular stress function model giving enhanced vortex growth," J. Non-Newton. Fluid Mech. **135**, 68–81 (2006).

[95] Wapperom, P., A. Leygue, and R. Keunings, "Numerical simulation of large amplitude oscillatory shear of a high-density polyethylene melt using the MSF model," J. Non-Newton. Fluid Mech. **130**, 63–76 (2005).

[96] Ahirwal, D., S. Filipe, I. Neuhaus, M. Busch, G. Schlatter, and M. Wilhelm, "Large amplitude oscillatory shear and uniaxial extensional rheology of blends from linear and long-chain branched polyethylene and polypropylene," J. Rheol. **58**, 635–658 (2014).

[97] Cziep, M. A., M. Abbasi, M. Heck, L. Arens, and M. Wilhelm, "Effect of molecular weight, polydispersity, and monomer of linear homopolymer melts on the intrinsic mechanical nonlinearity 3 Q 0 (ω) in MAOS," Macromolecules **49**, 3566–3579 (2016).

[98] Marrucci, G., and G. Ianniruberto, "Interchain pressure effect in extensional flows of entangled polymer melts," Macromolecules **37**, 3934–3942 (2004).

[99] Ball, R. C., and T. C. B. McLeish, "Dynamic dilution and the viscosity of star polymer melts," Macromolecules **22**, 1911–1913 (1989).

[100] Marrucci, G., Molecular modelling of flows of concentrated polymers, in *Transport Phenomena in Polymeric Systems* (Wiley, New York, 1989).

[101] Narimissa, E., V. H. Rolón-Garrido, and M. H. Wagner, "A hierarchical multi-mode MSF model for long-chain branched polymer melts part I: Elongational flow," Rheol. Acta **54**, 779–791 (2015).

[102] Narimissa, E., and M. H. Wagner, "A hierarchical multi-mode molecular stress function model for linear polymer melts in extensional flows," J. Rheol. **60**, 625–636 (2016).

[103] Narimissa, E., and M. H. Wagner, "A hierarchical multi-mode MSF model for long-chain branched polymer melts part III: Shear flow," Rheol. Acta **55**, 633–639 (2016).

[104] Narimissa, E., and M. H. Wagner, "From linear viscoelasticity to elongational flow of polydisperse polymer melts: The hierarchical multi-mode molecular stress function model," Polymer **104**, 204–214 (2016).

[105] Ianniruberto, G., and G. Marrucci, "Entangled melts of branched PS behave like linear PS in the steady state of fast elongational flows," Macromolecules **46**, 267–275 (2012).

[106] Narimissa, E., V. H. Rolón-Garrido, and M. H. Wagner, "A hierarchical multi-mode MSF model for long-chain branched polymer melts part II: Multiaxial extensional flows," Rheol. Acta **55**, 327–333 (2016).

[107] Kraft, M., Untersuchungen zur scherinduzierten rheologischen Anisotropie von verschiedenen Polyethylen-Schmelzen, Ph.D., Diss. Techn. Wiss., ETH Zürich, Zürich, 1996.

[108] Bastian, H., Non-linear viscoelasticity of linear and long-chain-branched polymer melts in shear and extensional flows, Ph.D. thesis, Universität Stuttgart, Stuttgart, 2001.

[109] Wingstrand, S. L., B. Shen, J. A. Kornfield, K. Mortensen, D. Parisi, D. Vlassopoulos, and O. Hassager, "Rheological link between polymer melts with a high molecular weight tail and enhanced formation of shish-kebabs," ACS Macro Lett. **6**, 1268–1273 (2017).

[110] Wingstrand, S. L., *On the Link Between Nonlinear Extensional Rheology and Morphology of Polymeric Fibers* (Technical University of Denmark (DTU), Copenhagen, 2017).

[111] Wingstrand, S. L., O. Hassager, D. Parisi, A. L. Borger, and K. Mortensen, "Flow induced crystallization prevents melt fracture of HDPE in uniaxial extensional flow," J. Rheol. **62**, 1051–1060 (2018).

[112] Raible, T., A. Demarmels, and J. Meissner, "Stress and recovery maxima in LDPE melt elongation," Polym. Bull. **1**, 397–402 (1979).

[113] Wagner, M. H., T. Raible, and J. Meissner, "Tensile stress overshoot in uniaxial extension of a LDPE melt," Rheol. Acta **18**, 427–428 (1979).

[114] Rolón-Garrido, V. H., and M. H. Wagner, "The damping function in rheology," Rheol. Acta **48**, 245–284 (2009).

[115] Laun, H. M., and H. Münstedt, "Elongational behaviour of a low density polyethylene melt—I. Strain rate and stress dependence of viscosity and recoverable strain in the steady-state. Comparison with shear data. Influence of interfacial tension," Rheol. Acta **17**, 415–425 (1978).

[116] Bach, A., H. K. Rasmussen, and O. Hassager, "Extensional viscosity for polymer melts measured in the filament stretching rheometer," J. Rheol. **47**, 429–441 (2003).

[117] Rasmussen, H. K., J. K. Nielsen, A. Bach, and O. Hassager, "Viscosity overshoot in the start-up of uniaxial elongation of low density polyethylene melts," J. Rheol. **49**, 369–381 (2005).

[118] Nielsen, J. K., H. K. Rasmussen, M. Denberg, K. Almdal, and O. Hassager, "Nonlinear branch-point dynamics of multiarm polystyrene," Macromolecules **39**, 8844–8853 (2006).

[119] Huang, Q., H. K. Rasmussen, A. L. Skov, and O. Hassager, "Stress relaxation and reversed flow of low-density polyethylene melts following uniaxial extension," J. Rheol. **56**, 1535–1554 (2012).

[120] Alvarez, N. J., J. M. R. Marín, Q. Huang, M. L. Michelsen, and O. Hassager, "Creep measurements confirm steady flow after stress maximum in extension of branched polymer melts," Phys. Rev. Lett. **110**, 168301 (2013).

[121] Hoyle, D., Q. Huang, D. Auhl, D. Hassell, H. K. Rasmussen, A. L. Skov, O. Harlen, O. Hassager, and T. McLeish, "Transient overshoot extensional rheology of long-chain branched polyethylenes: Experimental and numerical comparisons between filament stretching and cross-slot flow," J. Rheol. **57**, 293–313 (2013).

[122] Huang, Q., Molecular rheology of complex fluids, Ph.D. thesis, Technical University of Denmark, Copenhagen, 2013.

[123] Huang, Q., M. Mangnus, N. J. Alvarez, R. Koopmans, and O. Hassager, "A new look at extensional rheology of low-density polyethylene," Rheol. Acta **55**, 343–350 (2016).

[124] Burghelea, T. I., Z. Starý, and H. Münstedt, "On the "viscosity overshoot" during the uniaxial extension of a low density polyethylene," J. Non-Newton. Fluid Mech. **166**, 1198–1209 (2011).

[125] Rasmussen, H. K., and A. Fasano, "Flow and breakup in extension of low-density polyethylene," Rheol. Acta **57**, 317–325 (2018).

[126] Wagner, M. H., and V. H. Rolón-Garrido, "Verification of branch point withdrawal in elongational flow of pom-pom polystyrene melt," J. Rheol. **52**, 1049–1068 (2008).

[127] Masubuchi, Y., Y. Matsumiya, H. Watanabe, G. Marrucci, and G. Ianniruberto, "Primitive chain network simulations for pom-pom polymers in uniaxial elongational flows," Macromolecules **47**, 3511–3519 (2014).